Contact interaction, volume damageability and multicriterial limiting states of multielement tribo-fatigue systems

Sergei S. SHERBAKOV, Michael A. ZHURAVKOV and Leonid A. SOSNOVSKIY

Abstract. Methodology of the complex study of mechanical states of the tribo-fatigue system and its elements is presented. It includes sequential formulation and solution of the problems of determining system elements' contact interaction characteristics, spatial stress-strain state, volume damageability and multicriterial limiting states.

Keywords: tribo-fatigue, multielement system, boundary integral equations, contact, spatial stress-strain state, volume damageability, dangerous volume, cast iron.

2010 Mathematics Subject Classification: 74B05.

1. Introduction

One of the important modern problems of solid and contact mechanics is dedicated to construction of mechanical and mathematical models for the spatial stress-strain state of systems where the contact interaction with friction (rolling, sliding) between the bodies and non-contact (volumetric, including cyclic) deformation, at least, of one of the system elements are realized at a time. Such systems are under study in Tribo-Fatigue [14, 20, 28, 29, 30, 31] and are called active or tribo-fatigue systems (GOST 30638-99).

The characteristic examples of such systems are: roller/shaft, roller/ring, tube/ viscous fluid flow systems. These systems represent the models of such practically important systems as gearing, wheel/rail, pipeline section, etc.

S.S. Sherbakov
Belarusian State University, Minsk, Belarus, e-mail: sherbakovss@mail.ru

M.A. Zhuravkov
Ministry of Education of the Republic of Belarus, Minsk, Belarus, e-mail: zhuravkov@bsu.by

L.A. Sosnovskiy
Interdepartmental Laboratory "TRIBO-FATIGUE" Gomel-Grodno-Minsk, Belarus,
e-mail: sosnovskiy@tribo-fatigue.com

R. Wituła, B. Bajorska-Harapińska, E. Hetmaniok, D. Słota, T. Trawiński (eds.), *Selected Problems on Experimental Mathematics*. Wydawnictwo Politechniki Śląskiej, Gliwice 2017, pp. 17–38.

With regard to such objects, the problem of interaction of their elements in multi-element systems consisting of more than two contacting bodies arises. Another problem is the comprehensive assessment of mechanical states of a deformable system and its elements. It includes consistent statement and solution of problems of determination of spatial stress-strain state of system elements, their volumetric damageability states and multicriterial limiting states.

Analysis of tribo-fatigue systems requires the formulation of non-classical statement of boundary problems for simultaneous contacts of many bodies with initially unknown contact areas. Also such a statement should include the account of various non-contact boundary conditions for tension-compression, bending, torsion etc. It is expedient to implement this statement in terms of integral boundary equations and boundary element method [2, 3, 9, 32, 33 etc.] which proved to be efficient in solving contact problems. Since boundary element modeling unlike for example finite-element method involves discretization of only the boundary of a body then the problem dimensionality is reduced. In addition, boundary element calculations can be easily parallelized using graphics accelerators reducing the computation effort by tens and hundreds times.

It is generally difficult to obtain analytical solutions of contact problems in case of complex shapes of two interacting bodies. These solutions are aimed at finding contact surface parameters and determination and specific distributions of normal and tangential tractions at this surface. Boundary element method [6, 9, 12] based on using Green's functions [10, 33, 34, 36] in semi-analytical and numerical formulations is traditionally used to address these issues.

There is a specific problem accompanying the implementation of the boundary element method using the fundamental Boussinesque, Cerruti, Kelvin, etc. solutions for a concentrated force acting at a point in space or half-space. The neighborhood of such a point has the peculiarity: displacements and stresses tend to infinity there. Traditionally this problem is addressed by calculating the corresponding fields not in the actual point of concentrated load application but at spherical surface of its neighborhood [11, 37]. Another approach considers a pricewise solution comprised of the particular solutions for the surface and half-space under the surface [16, 17, 19, 20].

In addition to the above approaches the analytical solutions for distributed normal and tangential tractions over the surface of boundary element (linear, rectangular and triangular) may be used. These solutions are continuous in the space and half-space without peculiarities near the surface of distribution region [4, 35]. Such solutions may be superposed in order to obtain solutions for concrete distributions of surface tractions [1-8, 15, 38].

Basing on the known stress-strain state of tribo-fatigue system the models of the state of volumetric damageability and multicriterial limiting states should be constructed and applied. These models are necessary to forecast failures of the system at different limiting states like volumetric destruction under the separation into parts, surface damage under limiting wear with the account of force, temperature and friction loading in conditions of three-dimensional stress-strain state.

2. Resolving equations for a multielement tribo-fatigue system

Consider the problem for determination of the stress-strain state of each of the bodies of a multielement system consisting of n bodies which form two or more frictional contact pairs [14, 15, 38].

For some configuration of the kth body defined by its position in the space $\mathbf{r}^k$ at some time moment t, the relations responsible for the mechanical state of a body particle (elementary volume) should be satisfied. These are the continuity equation, the motion equation for a body particle, the dependence between displacements and strains, and Hooke's law [2, 8, 11, 34].

These equations are added with the first-kind boundary conditions if at the elastic body surface S_u the displacements $\overline{u}_i^{k^*}(\mathbf{r}^k)$ are assigned:

$$u_i^k = \overline{u}_i^{k^*}(\mathbf{r}^k, t) \tag{1}$$

and/or with the second-kind boundary conditions if at the body surface S_σ the force distribution $\bar{p}_i$ is assigned

$$\sigma_{ij}^k l_j^k = \bar{p}_i^k(r^k, t) \tag{2}$$

where l_j^k are the direction cosines.

In addition, the initial conditions can be defined

$$u_i^k\big|_{t=0} = u_i^{k0}, \quad \dot{u}_i^k\big|_{t=0} = \dot{u}_i^{k0}. \tag{3}$$

The interaction of n deformable bodies can be described in terms of the contact boundary conditions defined by the following relations:

$$\bar{\mathbf{u}}_l\big|_{S_u^{(lm)}} - \bar{\mathbf{u}}_m\big|_{S_u^{(lm)}} = \boldsymbol{\delta}_{lm}^{(u)}\left(\mathbf{r}^l, \mathbf{r}^m, t\right)\Big|_{S_u^{(lm)}}, \tag{4}$$

$$\mathbf{L}_\sigma\left(\bar{\mathbf{u}}_l\big|_{S_\sigma^{(lm)}}\right) - \mathbf{L}_\sigma\left(\bar{\mathbf{u}}_m\big|_{S_\sigma^{(lm)}}\right) = \bar{\mathbf{p}}_l\big|_{S_\sigma^{(lm)}} - \bar{\mathbf{p}}_m\big|_{S_\sigma^{(lm)}} = \boldsymbol{\delta}_{lm}^{(\sigma)}\left(\mathbf{r}^l, \mathbf{r}^m, t\right)\Big|_{S_u^{(lm)}}, \tag{5}$$

where $S^{(lm)}$ is the contact surface of bodies l and m, $S_\sigma^{(lm)} \subset S^{(lm)}$, $S_u^{(lm)} \subset S^{(lm)}$; $\bar{\mathbf{p}}_k = \{\bar{p}_1^k, \bar{p}_2^k, \bar{p}_3^k\} = \{\bar{p}_n^k, \bar{p}_{\tau 1}^k, \bar{p}_{\tau 2}^k\}$ and $\bar{\mathbf{u}}_k = \{\bar{u}_1^k, \bar{u}_2^k, \bar{u}_3^k\}$ are the vectors of contact tractions and displacements at the surface of the kth body, $\bar{p}_n^k = l_{nj}^k \bar{p}_j^k$ and $\bar{p}_{\tau 1}^k = l_{\tau 1 j}^k \bar{p}_j^k$, $\bar{p}_{\tau 2}^k = l_{\tau 2 j}^k \bar{p}_j^k$ are the normal and tangential components of contact tractions, $l_{nj}^k, l_{\tau 1 j}^k, l_{\tau 2 j}^k$ are the direction cosines; $\boldsymbol{\delta}_{lm}^{(u)} = \{\delta_{lm}^{(n,u)}, \delta_{lm}^{(\tau,u)}\}$, $\boldsymbol{\delta}_{lm}^{(\sigma)} = \{\delta_{lm}^{(n,\sigma)}, \delta_{lm}^{(\tau,\sigma)}\}$ are the displacement and tractions at the contact surface; $\bar{\mathbf{L}}_\sigma = \{L_{11}, L_{12}, L_{13}\}$ is the vector, whose components are given by the differential operators responsible for the dependence of stresses on strains. So, in the elastic statement these operators are of the following form:

$$L_{ij}(\mathbf{u}) = \mu\left(u_{i,j} + u_{i,j}\right) + \lambda u_{q,q}\delta_{ij}. \tag{6}$$

where δ_{ij} is the Kronecker delta, μ and λ are the Lamé constants.

Contact boundary conditions (4), (5) permit one to describe the interaction of both the components of one body with different mechanical properties (zonally homogeneous continuum):

$$\begin{aligned}\boldsymbol{\delta}_{lm}^{(u)}\left(\mathbf{r}^l,\mathbf{r}^m,t\right)\Big|_{S_u^{(lm)}} &= \bar{\mathbf{u}}_l\big|_{S_u^{(lm)}} - \bar{\mathbf{u}}_m\big|_{S_u^{(lm)}} = 0,\\ \boldsymbol{\delta}_{lm}^{(\sigma)}\left(\mathbf{r}^l,\mathbf{r}^m,t\right)\Big|_{S_u^{(lm)}} &= \bar{\mathbf{p}}_l\big|_{S_\sigma^{(lm)}} - \bar{\mathbf{p}}_m\big|_{S_\sigma^{(lm)}} = 0,\end{aligned} \tag{7}$$

and the elements of the system of bodies. In the last case, the value of tangential surface tractions according to the Coulomb law is limited and boundary conditions (4), (5) assume the form

$$\begin{aligned}\delta_{lm}^{(n,\sigma)}\left(\mathbf{r}^l,\mathbf{r}^m,t\right)\Big|_{S_u^{(lm)}} &= \bar{p}_n^l\big|_{S_\sigma^{(lm)}} - \bar{p}_n^m\big|_{S_\sigma^{(lm)}} = \bar{p}_n^{lm} - \bar{p}_n^{lm} = 0,\\ \delta_{lm}^{(\tau,\sigma)}\left(\mathbf{r}^l,\mathbf{r}^m,t\right)\Big|_{S_u^{(lm)}} &= \bar{p}_\tau^l\big|_{S_\sigma^{(lm)}} - \bar{p}_\tau^m\big|_{S_\sigma^{(lm)}} = \bar{p}_\tau^{lm} - \bar{p}_\tau^{lm} = 0,\ \ \bar{p}_\tau^{lm} \le f\bar{p}_n^{lm},\\ \delta_{lm}^{(n,u)}\left(\mathbf{r}^l,\mathbf{r}^m,t\right)\Big|_{S_u^{(lm)}} &= \bar{u}_n^l\big|_{S_u^{(lm)}} - \bar{u}_n^m\big|_{S_u^{(lm)}} = \bar{u}_n^{lm} - \bar{u}_n^{lm} = 0,\\ \delta_{lm}^{(\tau,u)}\left(\mathbf{r}^l,\mathbf{r}^m,t\right)\Big|_{S_u^{(lm)}} &= \bar{u}_\tau^l\big|_{S_u^{(lm)}} - \bar{u}_\tau^m\big|_{S_u^{(lm)}} = \begin{cases}\bar{u}_\tau^{lm} - \bar{u}_\tau^{lm} = 0,\ \bar{p}_\tau^{lm} < f\bar{p}_n^{lm},\\ \Delta\bar{u}_\tau^{lm} = var, \bar{p}_\tau^{lm} = f\bar{p}_n^{lm},\end{cases}\end{aligned} \tag{8}$$

where f is the friction coefficient, $\Delta\bar{u}_\tau^{lm}$ is the variable quantity to be defined.

If the non-conformal interaction is implemented between the bodies l and m, then the contact surface $S^{(lm)}$ is initially unknown. In this case, the sizes and shapes of contact regions, as well as the contact tractions distribution can be found with the use of the variation methods or the e matrix inversion method [8].

With regard to the contact interaction between the bodies l and m (components of a zonally homogeneous body), the system of resolving integral equations for the static equilibrium state at the surfaces of two bodies will be of the form [14, 15]:

$$\begin{Bmatrix}\bar{\mathbf{p}}_l^{(S)}\\ \bar{\mathbf{u}}_l^{(S)}\\ \boldsymbol{\delta}_{lm}^{(\sigma)}\\ \boldsymbol{\delta}_{lm}^{(u)}\\ \bar{\mathbf{p}}_m^{(S)}\\ \bar{\mathbf{u}}_m^{(S)}\end{Bmatrix} = \begin{bmatrix}\bar{\mathbf{L}}_\sigma\left(\mathbf{L}_u^{(S)}\right) & 0\\ \bar{\mathbf{L}}_u^{(S)} & 0\\ \bar{\mathbf{L}}_\sigma\left(\mathbf{L}_u^{(S)}\right) & -\bar{\mathbf{L}}_\sigma\left(\mathbf{L}_u^{(S)}\right)\\ \bar{\mathbf{L}}_u^{(S)} & -\bar{\mathbf{L}}_u^{(S)}\\ 0 & \bar{\mathbf{L}}_\sigma\left(\mathbf{L}_u^{(S)}\right)\\ 0 & \bar{\mathbf{L}}_u^{(S)}\end{bmatrix}\cdot\begin{Bmatrix}\bar{\mathbf{p}}_l\\ \bar{\mathbf{p}}_m\end{Bmatrix} + \begin{bmatrix}\bar{\mathbf{L}}_\sigma\left(\mathbf{L}_u^{(V)}\right) & 0\\ \bar{\mathbf{L}}_u^{(V)} & 0\\ \bar{\mathbf{L}}_\sigma\left(L_u^{(V)}\right) & -\bar{\mathbf{L}}_\sigma\left(\mathbf{L}_u^{(V)}\right)\\ \bar{\mathbf{L}}_u^{(V)} & -\bar{\mathbf{L}}_u^{(V)}\\ 0 & \bar{\mathbf{L}}_\sigma\left(\mathbf{L}_u^{(V)}\right)\\ 0 & \bar{\mathbf{L}}_u^{(V)}\end{bmatrix}\cdot\begin{Bmatrix}\mathbf{q}_l\\ \mathbf{q}_m\end{Bmatrix} \tag{9}$$

where $\mathbf{q}$ is the vector of volume forces at the interior point of the body, $\mathbf{L}_u^{(S)} = \left\{L_1^{(S,u)}, L_2^{(S,u)}, L_3^{(S,u)}\right\}$ and $\mathbf{L}_u^{(V)} = \left\{L_1^{(V,u)}, L_2^{(V,u)}, L_3^{(V,u)}\right\}$ are the vectors, whose components are represented by the integral operators for the action of surface and volume forces:

$$\begin{aligned}L_i^{(S,j)}\left(p_\varphi\right) &= \int_{S(\boldsymbol{\xi})} p_\varphi\left(\boldsymbol{\xi}\right) G_i^{(\varphi,j)}\left(\mathbf{x}-\boldsymbol{\xi}\right) dS\left(\boldsymbol{\xi}\right),\\ L_i^{(V,j)}\left(q_\varphi\right) &= \int_{V(\boldsymbol{\xi})} q_\varphi\left(\boldsymbol{\xi}\right) G_i^{(\varphi,j)}\left(\mathbf{x}-\boldsymbol{\xi}\right) dV\left(\boldsymbol{\xi}\right).\end{aligned} \tag{10}$$

where $j = u,\sigma$; $\varphi = n,\tau$, $G_i^{(n,u)}$, $G_i^{(\tau,u)}$ are the influence functions from the fundamental solutions (for example, Kelvin, Boussinesque, Cerruti problems) [4, 5, 8, 34, 36, 37].

Solution of the system (9) can be obtained by boundary element modeling [2, 6, 9, 10, 12, 33, 35]. This solution is based on finding the so-called, unknown "fictitious" boundary conditions expressed in terms of stresses $\bar{\mathbf{p}}_i$ corresponding to a set of the applied boundary conditions expressed both in terms of the stresses $\bar{\mathbf{p}}_i^{(S)}$, $\boldsymbol{\delta}_{lm}^{(\sigma)}$ and the displacements $\bar{\mathbf{u}}_l^{(S)}$, $\boldsymbol{\delta}_{lm}^{(u)}$.

After the calculation of the stresses $\bar{\mathbf{p}}_l$ the stress-strain state at the point $M(x_1, x_2, x_3)$ of the body l can be defined from the following relations for surface and volume forces

$$u_i^l = L_i^{(S,u)}\left(\bar{\mathbf{p}}_l\right) + L_i^{(V,u)}\left(\mathbf{q}_l\right), \quad \sigma_{ij}^l = L_{ij}\left(\mathbf{u}_i^l\right). \tag{11}$$

Unlike the model of zonally homogeneous continuum, the model for interaction of bodies (1)–(11) additionally considers the tangential surface forces p_τ for stick and slip regions. This allows taking into account the influence of friction forces to the formation on the mechanicals states of interacting bodies.

The system of equations for the interaction of n bodies is constructed similarly to system (9):

$$\begin{Bmatrix} \mathbf{C}_1 \\ \boldsymbol{\delta}_{lm}^{(\sigma)} \\ \boldsymbol{\delta}_{lm}^{(u)} \\ \mathbf{C}_2 \\ \boldsymbol{\delta}_{13}^{(\sigma)} \\ \boldsymbol{\delta}_{13}^{(u)} \\ \mathbf{C}_3 \\ \vdots \\ \boldsymbol{\delta}_{2n}^{(\sigma)} \\ \boldsymbol{\delta}_{2n}^{(u)} \\ \boldsymbol{\delta}_{3n}^{(\sigma)} \\ \boldsymbol{\delta}_{3n}^{(u)} \\ \mathbf{C}_n \end{Bmatrix} = \begin{pmatrix} \mathbf{A}_1 & 0 & 0 & \cdots & 0 \\ \mathbf{A}_{12} & -\mathbf{A}_{21} & 0 & & 0 \\ \bar{\mathbf{L}}_u^{(S)} & -\bar{\mathbf{L}}_u^{(S)} & 0 & & 0 \\ 0 & \mathbf{A}_2 & 0 & & 0 \\ \mathbf{A}_{13} & 0 & -\mathbf{A}_{31} & & 0 \\ \bar{\mathbf{L}}_u^{(S)} & 0 & -\bar{\mathbf{L}}_u^{(S)} & & 0 \\ 0 & 0 & \mathbf{A}_3 & & 0 \\ \vdots & \vdots & \vdots & \ddots & \vdots \\ 0 & \mathbf{A}_{2n} & 0 & & -\mathbf{A}_{n2} \\ 0 & \bar{\mathbf{L}}_u^{(S)} & 0 & & -\bar{\mathbf{L}}_u^{(S)} \\ 0 & 0 & \mathbf{A}_{3n} & & -\mathbf{A}_{n3} \\ 0 & 0 & \bar{\mathbf{L}}_u^{(S)} & & -\bar{\mathbf{L}}_u^{(S)} \\ 0 & 0 & 0 & \cdots & \mathbf{A}_n \end{pmatrix} \begin{Bmatrix} \bar{\mathbf{p}}_1 \\ \bar{\mathbf{p}}_2 \\ \bar{\mathbf{p}}_3 \\ \vdots \\ \bar{\mathbf{p}}_n \end{Bmatrix} + \begin{pmatrix} \mathbf{B}_1 & 0 & 0 & \cdots & 0 \\ \mathbf{B}_{12} & -\mathbf{B}_{21} & 0 & & 0 \\ \bar{\mathbf{L}}_u^{(V)} & -\bar{\mathbf{L}}_u^{(V)} & 0 & & 0 \\ 0 & \mathbf{B}_2 & 0 & & 0 \\ \mathbf{B}_{13} & 0 & -\mathbf{B}_{31} & & 0 \\ \bar{\mathbf{L}}_u^{(V)} & 0 & -\bar{\mathbf{L}}_u^{(V)} & & 0 \\ 0 & 0 & \mathbf{B}_3 & & 0 \\ \vdots & \vdots & \vdots & \ddots & \vdots \\ 0 & \mathbf{B}_{2n} & 0 & & -\mathbf{B}_{n2} \\ 0 & \bar{\mathbf{L}}_u^{(V)} & 0 & & -\bar{\mathbf{L}}_u^{(V)} \\ 0 & 0 & \mathbf{B}_{3n} & & -\mathbf{B}_{n3} \\ 0 & 0 & \bar{\mathbf{L}}_u^{(V)} & & -\bar{\mathbf{L}}_u^{(V)} \\ 0 & 0 & 0 & \cdots & \mathbf{B}_n \end{pmatrix} \begin{Bmatrix} \mathbf{q}_1 \\ \mathbf{q}_2 \\ \mathbf{q}_3 \\ \vdots \\ \mathbf{q}_n \end{Bmatrix} \tag{12}$$

where $\mathbf{A}_{lm}$, $\mathbf{B}_{lm}$ and $\mathbf{C}_l$, $\mathbf{A}_l$, $\mathbf{B}_l$ are the short designations of operators and groups of operators.

Now consider the construction of the system of resolving equations with regard to the wave effects [1], for example, with the use of the fundamental solution of the Kelvin problem in the dynamic statement [7].

In this case, the operators similar to (10) assume the form

$$L_i^{(S,t,j)}\left(p_\varphi(t)\right) = \int_0^t \int_{S(\xi,\tau)} p_\varphi(\xi,\tau)\, G_i^{(\varphi,j)}(\mathbf{x}-\xi,t,\tau)\, dS(\xi,\tau)\, d\tau \tag{13}$$

$$L_i^{(V,t,j)}\left(q_\varphi(t)\right) = \int_0^t \int_{V(\xi,\tau)} q_\varphi(\xi,\tau)\, G_i^{(\varphi,j)}(\mathbf{x}-\xi,t,\tau)\, dV(\xi,\tau)\, d\tau \tag{14}$$

With regard to operators (13) and (14), system (9) will be the following

$$\left\{\begin{array}{c}\bar{\mathbf{p}}_l^{(S)}(t)\\ \bar{\mathbf{u}}_l^{(S)}(t)\\ \boldsymbol{\delta}_{lm}^{(\sigma)}(t)\\ \boldsymbol{\delta}_{lm}^{(u)}(t)\\ \bar{\mathbf{p}}_m^{(S)}(t)\\ \bar{\mathbf{u}}_m^{(S)}(t)\end{array}\right\} = \begin{bmatrix}\bar{\mathbf{L}}_\sigma\left(\mathbf{L}_u^{(S,t)}\right) & 0\\ \bar{\mathbf{L}}_u^{(S,t)} & 0\\ \bar{\mathbf{L}}_\sigma\left(L_u^{(S,t)}\right) & -\bar{\mathbf{L}}_\sigma\left(L_u^{(S,t)}\right)\\ \bar{\mathbf{L}}_u^{(S,t)} & -\bar{\mathbf{L}}_u^{(S,t)}\\ 0 & \bar{\mathbf{L}}_\sigma\left(L_u^{(S,t)}\right)\\ 0 & \bar{\mathbf{L}}_u^{(S,t)}\end{bmatrix}\cdot\left\{\begin{array}{c}\bar{\mathbf{p}}_l(t)\\ \bar{\mathbf{p}}_m(t)\end{array}\right\}+$$
$$+\begin{bmatrix}\bar{\mathbf{L}}_\sigma\left(L_u^{(V,t)}\right) & 0\\ \bar{\mathbf{L}}_u^{(V,t)} & 0\\ \bar{\mathbf{L}}_\sigma\left(\mathbf{L}_u^{(V,t)}\right) & -\bar{\mathbf{L}}_\sigma\left(\mathbf{L}_u^{(V,t)}\right)\\ \bar{\mathbf{L}}_u^{(V,t)} & -\bar{\mathbf{L}}_u^{(V,t)}\\ 0 & -\bar{\mathbf{L}}_\sigma\left(\mathbf{L}_u^{(V,t)}\right)\\ 0 & -\bar{\mathbf{L}}_u^{(V,t)}\end{bmatrix}\cdot\left\{\begin{array}{c}\mathbf{q}_l(t)\\ \mathbf{q}_m(t)\end{array}\right\} \tag{15}$$

The system of the resolving equations for n bodies in the dynamic statement is formulated using equations (15) similarly to system (12).

3. Change of contact pressure due to non-contact bending

Consider the example of calculation of contact pressure with regard to non-contact (volume) deformation (Figure 1a). As an object of study, let us take a roller/shaft system that is acted upon by contact F_N and non-contact F_b forces (Figure 1b). This model is used in wear-fatigue tests for mechano-rolling fatigue [14, 15, 22, 30].

From Figure 1b it is seen that the surfaces of contacting bodies are bounded by the second-order surfaces, therefore, to determine contact pressure, one could confine oneself to Hertz's theory. Yet, since during long fatigue loading the cases of contact of bodies with arbitrary-shape surfaces are most probable, it is preferable to use more general methods of numerical modeling for contact pressure calculation. Our calculation uses the matrix inversion technique, whose description can be found, for example, in [8].

Elastic displacements of the corresponding points of two surfaces obey the relation

$$\bar{u}_{z1}+\bar{u}_{z2}+\left[z_1(x,y)-z_2(x,y)\right]-\delta=\bar{u}_{z1}+\bar{u}_{z2}+h(x,y)-\delta\left\{\begin{array}{l}=0,(x,y)\in S,\\ >0,(x,y)\notin S,\end{array}\right. \tag{16}$$

where δ is the approach of contacting bodies, $z_1(x,\ y)$ and $z_2(x,\ y)$ are the equations of body surfaces, and S is the contact region.

Numerical modeling of contact interaction will be performed for the following parameters: $v_1 = v_2 = 0.3$, $E_1 = E_2 = 2.01 \cdot 10^{11}$Pa, $R_{11} = 0.005$m, $R_{12} = 0.05$m, $R_{21} = 0.01$m, $R_{22} = 0.01$m (see Figure 1b).

A contact load will be assigned by (a) the force $F_N = 2000\text{H}$ and (b) the bodies approach $\delta = 2.723 \cdot 10^{-5}\text{m}$, corresponding to the mentioned value of F_N following Hertz's theory. The ratio of the contact ellipse half-axes $a/b = 0.89$. Computational domain sizes are: $1.5a \leq x$ and $y \leq 1.5a$ where $a = 5.296 \cdot 10^{-4}\text{m}$. The domain was partitioned into 21×21 square elements.

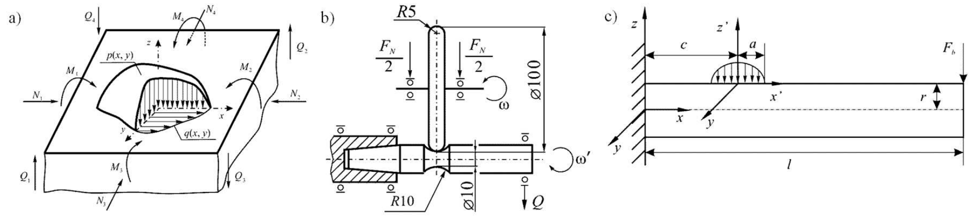

Fig. 1. Schemes of tribo-fatigue system loading (a), wear-fatigue tests (b), shaft loading (c)

The obtained numerical solution for the contact pressure distribution was compared with the Hertzian analytical solution for the distribution of elliptic type.

According to the following formulas

$$\varepsilon_i = \frac{p_i^H - p_i}{p_0^H}, \quad \varepsilon_{\max} = \max_i |\varepsilon_i|, \quad \varepsilon_{avg} = \frac{1}{n}\sum_{i=1}^{n} |\varepsilon_i| \tag{17}$$

calculation errors in comparison with analytical solution were $\varepsilon_{max} = 5.9 \cdot 10^{-2}$ and $\varepsilon_{avg} = 4 \cdot 10^{-3}$.

Vertical displacements of the contact region due to the action of non-contact tension-compression or bending by load F_b are respectively [14, 15]:

$$\bar{u}_z^{(b1)} = -\frac{\nu_2}{E_2}\sigma_{xx}^{(b1)} R_2, \quad \bar{u}_z^{(b2)} = -\frac{\nu_2}{2E_2}\sigma_{xx}^{(b2)} R_2. \tag{18}$$

Figure 2a shows that the contact force F_N based on $F_N^{(c)} = 2000\text{H}$ depending on the non-contact stresses at the contact region center σ_a based on $\sigma_a^{(\max)} = 6.4 \cdot 10^8$ Pa varies approximately from $+60\%$ to -50% at tension-compression and approximately from $+27\%$ to -25% at bending.

Figure 2b demonstrates that at mechano-rolling fatigue tests, the variation of the rolling fatigue coefficient is somewhat higher in the compression zone as against the one in the tension zone. This is in a qualitative agreement with the calculation results presented (see Figures 2a and b).

Another qualitative verification of the calculations is provided by test results (see Figures 3 and 4) for the roller/shaft system loading scheme according to Figure 1b obtained from the SI machines [23, 26, 30]. Four fatigue curves are plotted from the experimental data (see Figure 3).

The limiting state criterion in mechanical fatigue tests is the disintegration of a specimen into pieces. The limiting state criterion in rolling fatigue tests is the critical density of pittings at the rolling surface. The limiting state in tests for mechano-rolling fatigue is determined by the damage and fracture criteria typical for mechanical and rolling fatigue tests.

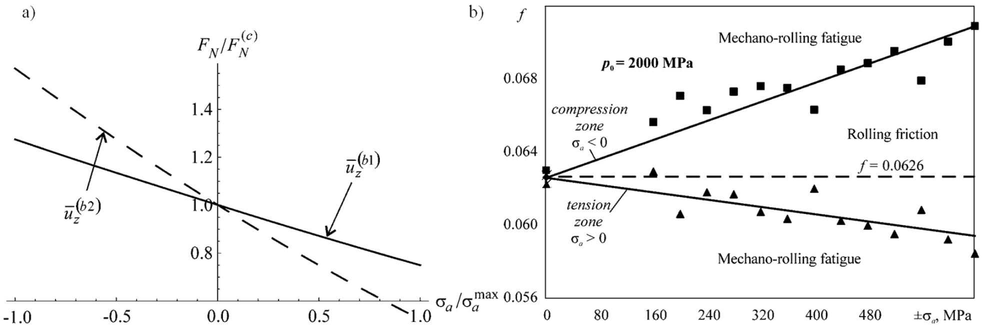

Fig. 2. Dependence between contact load and the level of stresses due to non-contact deformation (a), experimental dependence between the rolling friction coefficient in the roller/shaft system and the non-contact stresses in the contact region (b)

The fatigue limits $(\sigma_{-1}, p_f, \sigma_{-1p}, p_{f\sigma})$, the slope parameters of the left branch of the fatigue curves $(m_\sigma, m_p, m_{\sigma p}, m_{p\sigma})$, and the abscissas of the inflection points of the fatigue curves $(N_{\sigma G}, N_{pG}, N_{\sigma pG}, N_{p\sigma G})$ are determined in all four cases (see Figure 3). Note that σ_{-1} is the limiting stress for the specimen (shaft) undergoing cyclic bending with rotation. Under mechano-rolling fatigue, σ_{-1p} is the same limiting stress for a specimen being subjected to a contact pressure p_0. Similarly, p_f is the limiting contact pressure for the friction pair under rolling fatigue. Lastly, in mechano-rolling fatigue, $p_{f\sigma}$ is the same limiting contact pressure as considering the influence of stresses σ_a due to bending.

Figure 4 shows the first multi-criteria diagram of the limiting states of a Tribo-Fatigue system with mechano-rolling fatigue.

The analysis of fatigue curves in Figures 3 and the diagram $ABCD$ (see Figure 4) allows the following basic conclusions to be made.

The fatigue limit of a specimen can increase by a factor of up to 1.5 or 1.6, provided that rolling occurs simultaneously (the direct effect – portion AB).

The critical (limiting) pressure for rolling can increase by a factor of up to 1.20 or 1.25, if cyclic stresses are simultaneously imposed upon the specimen (the back effect – portion DC).

Within the optimum contact pressure range ($p_0 = 400 - 1.300MPa$), the rolling wear process leads to a significant rise of the system reliability in terms of fatigue resistance; for this reason, it would be detrimental to strive for wear-free friction in this case.

At cyclic loading under the optimum conditions($\sigma_a \approx 50 - 100MPa$), tensile stresses are favourable because they promote a considerable rise in the system reliability in terms of rolling friction resistance. The latter conclusion about positive effect of tensile stresses in the neighbourhood of the contact area on contact parameters is also in the qualitative agreement with the calculation results (see Figure 2a) showing the decrease of contact force in the zone of tensile stresses due to the action non-contact bending load.

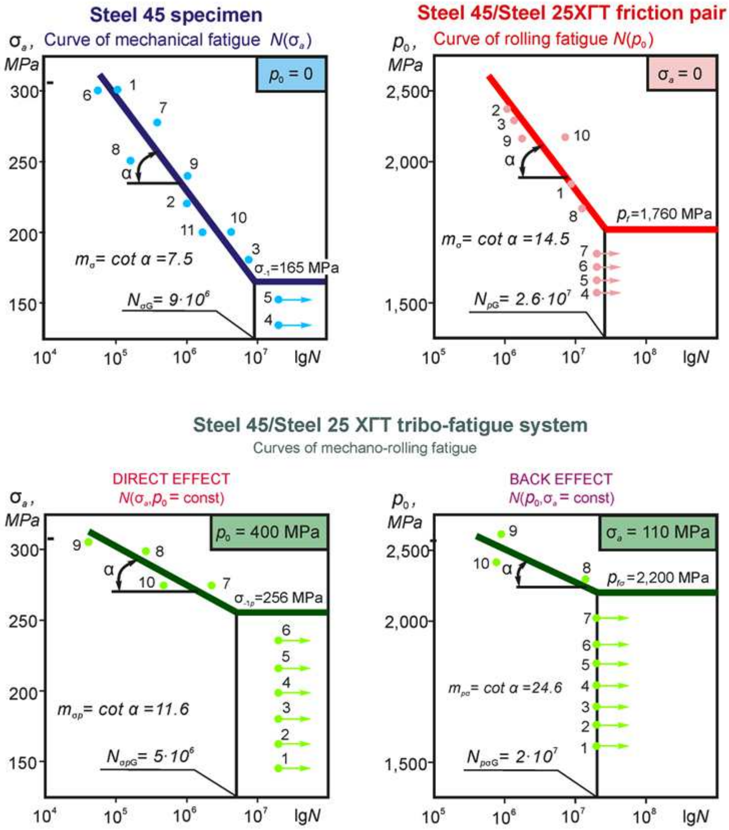

Fig. 3. Experimental curves of roller-shaft system under conditions of mechanical, rolling and mechano rolling fatigue [23, 26, 30]

4. Dangerous volumes as the model of damageability

Mechanical state of the system at a point (elementary volume) can be assessed as the limiting one when some mechanical parameters reach their limiting values.

According to the model of a deformable solid with dangerous volume [13, 14, 18, 24, 25, 30] dangerous volumes represent three-dimensional regions of a solid body, in which stresses come to a damaging level. In essence, dangerous volumes are a nonlocal characteristic of the distribution of physical-mechanical properties to be defined by the material structure.

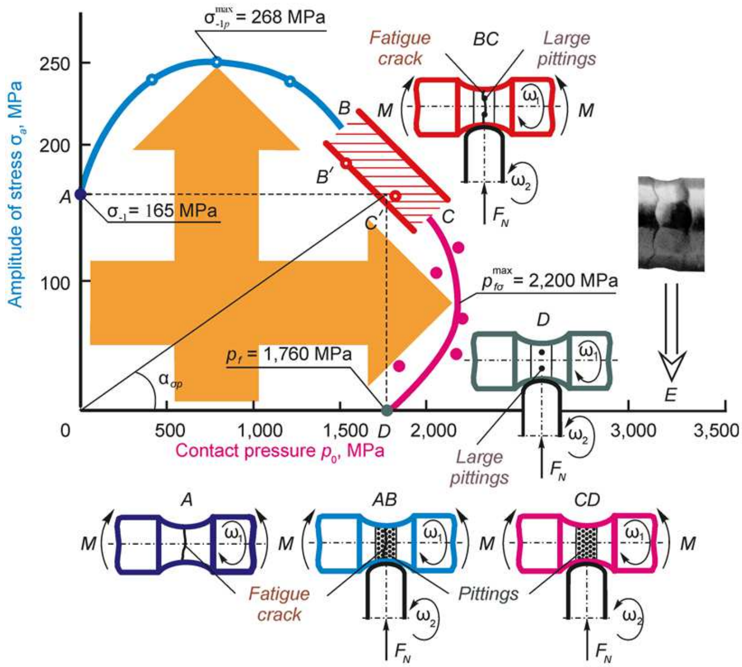

Fig. 4. Multi-criteria diagram of the limiting states of steel 25 XГT (roller)/steel 45 (shaft) tribo-fatigue system under mechano-rolling fatigue [23, 26, 30]

Consider the mechanical parameter φ, whose concretization can be represented by the stress tensor σ, the strain tensor ε, as well as the specific potential deformation energy u. In the general case, when the limiting load $F_{*\mathrm{lim}}$ acts upon the tribo-fatigue system, consider the limiting value of the mechanical parameter $\varphi^{(*\mathrm{lim})}$.

Passing directly to the damageability assessment, for an anisotropic deformable solid body the limiting value of the mechanical parameter for each independent tensor component $\varphi_{ij}^{(\pm *\mathrm{lim})}$, i, $j = x$, y, z, for each principal component $\varphi_{i}^{(\pm *\mathrm{lim})}$, $i = 1, 2, 3$ and the intensity $\varphi_{\mathrm{int}}^{(*\mathrm{lim})}$, when the tribo-fatigue system is acted upon by the limiting load $F_{*\mathrm{lim}}$ (causing the three-dimensional stress-strain state in the general case), is defined as follows [14,30,31]:

$$\begin{aligned} \varphi_{ij}^{(\pm *\mathrm{lim})} &= \underset{dV}{extr}\left[\varphi_{ij}\left(F_{*\mathrm{lim}}\, dV\right)\right], \quad \varphi_{i}^{(\pm *\mathrm{lim})} = \underset{dV}{extr}\left[\varphi_{i}\left(F_{*\mathrm{lim}}\, dV\right)\right], \\ \varphi_{int}^{(*\mathrm{lim})} &= \max_{dV}\left[\varphi_{int}\left(F_{*\mathrm{lim}}\, dV\right)\right], \end{aligned} \tag{19}$$

where dV is the elementary volume of a loaded body, $extr(y) = \begin{cases} \max(y), \text{ if } y \geq 0, \\ \min(y) \text{ if } y < 0. \end{cases}$

According to (19), the limiting values of stresses or strains of an anisotropic deformable solid body are the extreme (maximum for tensile stresses or strains and minimum for compressive stresses or strains) values of the distributions of the parameter φ.

Similarly, for an isotropic deformable solid state we define the limiting normal and tangential values of $\varphi_n^{(*\lim)}$ and $\varphi_\tau^{(*\lim)}$ of the tensor $\varphi_{ij}^{(\pm *\lim)}$, as well as the limiting principal components $\varphi_i^{(*\lim)}$ of stresses (strains), the limiting intensity of stresses (strains) $\varphi_{int}^{(*\lim)}$ and the limiting specific potential deformation energy $u^{(*\lim)}$:

$$\begin{aligned}
\varphi_n^{(*\lim)} &= \max_{dV,i}\left(\left|\varphi_{ii}\left(F_{*\lim},\ dV\right)\right|\right), \quad i = x, y, z, \\
\varphi_q^{(*\lim)} &= \max_{dV}\left(\left|\varphi_q\left(F_{*\lim},\ dV\right)\right|\right), \\
\varphi_\tau^{(*\lim)} &= \max_{dV,i,j}\left(\left|\varphi_{ij}\left(F_{*\lim},\ dV\right)\right|\right), \quad i,j = x, y, z, \quad i \neq j, \\
u^{(*\lim)} &= \max_{dV}\left(\left|u\left(F_{*\lim},\ dV\right)\right|\right),
\end{aligned} \tag{20}$$

where $q = \{i, int\}$.

If the mechanical parameter φ is considered within each elementary volume dV of the body, then in the general case, to describe the changes in values of φ in comparison with the limiting value, it is possible to introduce the tensors (matrices) of relative damaging mechanical parameters (component, principal, octahedral, energy):

$$\psi_q = \varphi_q / \varphi_q^{(*\lim)}, \quad \psi_u = u / u^{(*\lim)} \tag{21}$$

where q={ij,i,int}, ψ_{ij}, ψ_i, ψ_{int}, ψ_u are generally speaking probabilistic in nature since under loading both the values of φ_{ij}, φ_i, φ_{int}, u, as well as the limiting values of the mechanical parameter $\varphi_k^{(*\lim)}$, $\varphi_i^{(*\lim)}$, $\varphi_{int}^{(*\lim)}$,$u^{(*\lim)}$ are the random values with the corresponding distribution functions.

Unlike the studied single-axis stresses state [30], the definition of dangerous volumes for the considered three-axial stress-strain state is more intricate. The criterion conditions for the limitation of dangerous volumes and the formula for calculation of its values in the last case will be of the form [14, 30, 31]

$$V_q = \left\{\, dV / \psi_q \geq 1,\ dV \subset V_k \right\}, \quad V_q = \int_{\psi_q \geq 1} dV \tag{22}$$

where q={ij,i,int,u}, V_k is the working volume of a deformable solid body.

The simplest functions for the damageability accumulation in time per unit volume and total volume will be, respectively:

$$d\Psi_q^{(t)} = \int_t \psi_q\left(t\right) dt, \quad \text{and} \quad \Psi_q^{(V,t)} = \int_{\psi_q \geq 1} \int_t \psi_q\left(V, t\right) dt dV \tag{23}$$

For the damageability to be assessed integrally, the values of the volume-averaged damageability and its change in time can be used

$$\Psi_q^{(V_{av})} = \frac{1}{V_q} \int_{\psi_q \geq 1} \psi_q (V) \, dV, \quad \Psi_q^{(V_{av},t)} = \frac{1}{V_{ij}} \int_{\psi_q \geq 1} \int_t \psi_q (V,t) \, dt dV. \tag{24}$$

Functions (22)–(24) allow one to analyze in time the system damageability in different spatial regions.

5. Generalized criterion of the limiting state of the tribo-fatigue system

Model of multicriterial limiting states of the tribo-fatigue is created in order to allow forecasting failures of system elements according to various criteria of a limiting state: volume destruction under the separation into parts, surface damage under limiting wear with the account of the force, temperature and friction loading in conditions of spacial stress-strain state.

The generalized criterion of the limiting state of the tribo-fatigue system based on its united stress state is formulated as follows [14, 30]:

$$u_\Sigma^{eff}(\sigma^{(V,W)},\ \varepsilon^{(V,W)},\ T_\Sigma,\ Ch,\ \Lambda(V),\ m_k) = u_0. \tag{25}$$

where it is assumed that the value of the effective energy u_Σ^{eff} is defined in terms of the tensors of stresses σ and strains ε, as well as in terms of the temperature of all heat sources T_Σ, whereas u_0 should be interpreted as the initial activation energy of the destruction process.

It was shown that the quantity u_0 approximately coincides with the sublimation heat for metals or crystals with ionic bonds and also with the activation energy of thermal destruction for polymers. Stress and strain tensors with an index V are caused by the action of volume loads (general cases of three-dimensional bending, twisting, tension-compression) and those with an index W – by the contact interaction of system elements.

To determine the effective energy, consider the work of internal forces in the elementary volume dV of the tribo-fatigue system.

In the general case, the differential of the work of the internal forces and the temperature dT_Σ can be written with regard to the rule of disclosing the biscalar product of the stress and strain tensors σ and ϵ [2, 7, 8, 37]:

$$\begin{aligned} du = \sigma_{ij} \cdot \cdot d\varepsilon_{ij} + kdT_\Sigma = \begin{pmatrix} \sigma_{xx} & \sigma_{xy} & \sigma_{xz} \\ \sigma_{yx} & \sigma_{yy} & \sigma_{yz} \\ \sigma_{zx} & \sigma_{zy} & \sigma_{zz} \end{pmatrix} \cdot \cdot \begin{pmatrix} d\varepsilon_{xx} & d\varepsilon_{xy} & d\varepsilon_{xz} \\ d\varepsilon_{yx} & d\varepsilon_{yy} & d\varepsilon_{yz} \\ d\varepsilon_{zx} & d\gamma_{zy} & d\varepsilon_{zz} \end{pmatrix} + kdT_\Sigma = \\ = \sigma_{xx} d\varepsilon_{xx} + \sigma_{yy} d\varepsilon_{yy} + \sigma_{zz} d\varepsilon_{zz} + \sigma_{xy} d\varepsilon_{xy} + \sigma_{xz} d\varepsilon_{xz} + \sigma_{yz} d\varepsilon_{yz} + kdT_\Sigma \end{aligned} \tag{26}$$

or in terms of principal stresses and strains

$$du = \sigma_i \cdot \cdot d\varepsilon_i + kdT_\Sigma = \sigma_1 d\varepsilon_1 + \sigma_2 d\varepsilon_2 + \sigma_3 d\varepsilon_3 + kdT_\Sigma \tag{27}$$

here k is the Boltzmann constant.

We will proceed from the idea that according to [14, 26] the essential role in the formation of wear-fatigue damage is played by both normal and tangential stresses that cause the processes of shear (due to friction) and separation (due to tension-compression). In order to meet the requirements of independence of the state equations on the system of coordinates it is reasonable to represent the tensor σ_{ij} in terms of principal stresses in two parts: deviatoric stress tensor σ_τ considered as the part of friction-shear stresses, or, briefly, the shear part and volumetric stress tensor σ_n considered as the part of normal stresses (tension-compression), or the tear part:

$$\begin{aligned}
\sigma_n &= \frac{1}{3}\left(\sigma_1+\sigma_2+\sigma_3\right), \\
\sigma_\tau = \sigma_{ij}-\sigma_n\delta_{ij} &= \begin{pmatrix} \sigma_1-\sigma_n & 0 & 0 \\ 0 & \sigma_2-\sigma_n & 0 \\ 0 & 0 & \sigma_3-\sigma_n \end{pmatrix} = \\
&= \frac{1}{3}\begin{pmatrix} 2\sigma_1-\sigma_2-\sigma_3 & 0 & 0 \\ 0 & 2\sigma_2-\sigma_1-\sigma_3 & 0 \\ 0 & 0 & 2\sigma_3-\sigma_1-\sigma_2 \end{pmatrix},
\end{aligned} \tag{28}$$

So in (27) the connection between energy increment du, stresses, strains and temperature taking into account (28) will have the following form:

$$\begin{aligned}
du &= \sigma_i\cdot\cdot d\varepsilon_i + kdT_\Sigma = \sigma_n de + \sigma_\tau\cdot\cdot d\varepsilon_i + kdT_\Sigma = \sigma_n de + \sigma_\tau\cdot\cdot d\varepsilon_i + kdT_\Sigma \\
&= \frac{1}{3}\left(\sigma_1+\sigma_2+\sigma_3\right)\left(d\varepsilon_1+d\varepsilon_2+d\varepsilon_3\right) \\
&+ \frac{1}{3}\left[\left(2\sigma_1-\sigma_2-\sigma_3\right)d\varepsilon_1+\left(2\sigma_2-\sigma_1-\sigma_3\right)d\varepsilon_2+\left(2\sigma_3-\sigma_1-\sigma_2\right)d\varepsilon_3\right]+kT_\Sigma \\
&= du_n + du_\tau + du_T,
\end{aligned} \tag{29}$$

where $de = \ d\varepsilon_1 + d\varepsilon_2 + d\varepsilon_3$ – volume expansion increment in terms of principal strains.

From the total deformation energy we will take its effective part. To do this, we will introduce the coefficients $A_n(V)$, $A_\tau(V)$ and $A_T(V)$ according to [14, 26, 30] of relevant dimensionality that will specify the fraction of absorbed energy (spent for damage production):

$$du_\Sigma^{eff} = \Lambda_{M\backslash T}(V)\left\{\Lambda_{\tau\backslash n}(V)\left[A_n(V)\sigma_n d_n e + A_\tau(V)\sigma_\tau\cdot\cdot d\varepsilon_i\right] + A_T(V)kdT_\Sigma\right\}, \tag{30}$$

where $\Lambda_{\tau\backslash n}(V)$, $\Lambda_{M\backslash T}(V)$ are the functions of interaction between the energies of different nature [14, 26, 30]: shear and separation energies (subscript $\tau\backslash n$), mechanical and thermal energies (subscript $M\backslash T$).

The fact that generally speaking, the coefficients A can be different for different points of the volume V enables one to take into account the nonuniformity of continuum.

Criterion (25) with regard to (30) assumes the form

$$\Lambda_{M\backslash T}\left(V\right)\left\{\Lambda_{\tau\backslash n}\left(V\right)\left[du_n^{eff}+du_\tau^{eff}\right]+du_T^{eff}\right\} = u_0. \tag{31}$$

In the case of a linear relationship between stresses and strains, expressions (30) and (31) will be of the following form

$$\begin{aligned} u_{\Sigma}^{eff} &= \Lambda_{M\backslash T}(V)\left\{\Lambda_{\tau\backslash n}(V)\left[A_n(V)\frac{1}{2}\sigma_n e + A_\tau(V)\frac{1}{2}\sigma_\tau\cdot\cdot\varepsilon_i\right] + A_\tau(V)\,kT_\Sigma\right\} \\ &= \Lambda_{M\backslash T}(V)\left\{\Lambda_{\tau\backslash n}(V)\left[A_n(V)\frac{1}{6}(\sigma_1+\sigma_2+\sigma_3)(\varepsilon_1+\varepsilon_2+\varepsilon_3)\right.\right. \\ &\left.+ A_\tau(V)\frac{1}{2}\left(\frac{2\sigma_1-\sigma_2-\sigma_3}{3}\varepsilon_1 + \frac{2\sigma_2-\sigma_1-\sigma_3}{3}\varepsilon_2 + \frac{2\sigma_3-\sigma_1-\sigma_2}{3}\varepsilon_3\right)\right] \\ &\left.+ A_\tau(V)\,kT_\Sigma\right\} = \Lambda_{M\backslash T}(V)\left\{\Lambda_{\tau\backslash n}(V)\left[A_n(V)\frac{(1-2\nu)}{6E}(\sigma_1+\sigma_2+\sigma_3)^2\right.\right. \\ &\left.+ A_\tau(V)\frac{1+\nu}{6E}\left[(\sigma_1-\sigma_2)^2+(\sigma_1-\sigma_3)^2+(\sigma_2-\sigma_3)^2\right]\right] \\ &\left.+ A_\tau(V)\,kT_\Sigma\right\} = u_0. \end{aligned} \tag{32}$$

where $e=\varepsilon_1+\varepsilon_2+\varepsilon_3$, E is modulus of elasticity, ν is Poisson's ratio.

Thus, criterion (25) can be given as follows:

$$u_{\Sigma}^{eff}=\left\{\left[u_n^{eff}(\sigma_n^{(V,W)},e^{(V,W)})+u_\tau^{eff}(\sigma_\tau^{(V,W)},\varepsilon_i^{(V,W)})\right]\Lambda_{\tau\backslash n}+u_T^{eff}\right\}\Lambda_{M\backslash T}=u_0, \tag{33}$$

or in damageability terms:

$$\psi_u^{eff}=u_{\Sigma}^{eff}/u_0=1. \tag{34}$$

The following effective energy characteristics of damageability can be introduced. These are the integral effective energy damageability (within the dangerous volume) and the mean energy damageability (at each point of the dangerous volume).

$$\Psi_u^{(eff)}=\int_{\psi_u^{eff}(dV)\geq 1}\psi_u^{eff}dV,\quad \Psi_u^{(eff,V_{av})}=\frac{1}{V_u}\int_{\psi_u^{eff}(dV)\geq 1}\psi_u^{eff}dV. \tag{35}$$

The time accumulation of effective energy damageability (within the dangerous volume) is described by the equations:

$$\Psi_u^{(eff,t)}=\int_{\psi_u^{eff}(dV)\geq 1}\int_t\psi_u^{eff}dtdV,\quad \Psi_u^{(eff,V_{av},t)}=\frac{1}{V_u}\int_{\psi_u^{eff}(dV)\geq 1}\int_t\psi_u^{eff}dtdV. \tag{36}$$

The damageability of the tribo-fatigue system can be described and analyzed with the use of formulas (35), (36) from the most general energy viewpoint.

The practical workability of the energy criterion of tribo-fatigue systems is supported by the example of the isothermal mechanical fatigue analysis according to equation (33). So, it is easy to obtain (at $\sigma=\sigma_{-1T}$) an equation for assessment of thermal-mechanical fatigue resistance. For particular cases of different-class materials the testing was made using the appropriate experimental results of many authors (more than 300 tests) [14, 30]. It has revealed that for the temperature dependence of the tensile strength limits the correlation coefficient is very high being no less than $r=0.722$, but in most of the cases it exceeds $r=0.9$.

6. Stress-strain and damageability states of the typical tribo-fatigue system

Consider the comparison of one of the solutions for the traditional contact problem for a roller/roller pair at elliptical contact pressure distributions and the similar solution for the tribo-fatigue roller/shaft system (Figures 1a and b) where the shaft is additionally bent by a non-contact force [14, 16, 17, 19, 27, 31]. The bending load is applied in the way that the region of tensile stresses is formed in the vicinity of the contact area.

When the stress state was studied, the calculation was made for the region $z \in [0; 1.5a]$, $x \in [-1.5a; 1.5a]$, $y \in [-1.5a; 1.5a]$ for $20 \times 39 \times 39$ points under action of the non-contact load $F_b = 1.2p_0\frac{4(1+\nu)J}{12r^2}$ (where p_0 is the maximum contact pressure, r is the shaft radius, J is the shaft moment of inertia), the shaft length is $12r$. The following values were taken for material properties and geometric characteristics of the system: $E_1 = E_2 = 2.01 \cdot 10^{11}$Pa, $\nu_1 = \nu_2 = 0.3$, R_{11}, friction coefficient $f = 0.2$, ratio of contact ellipse half-axes $b/a = 0.5$. Some calculation results are shown in Figure 5.

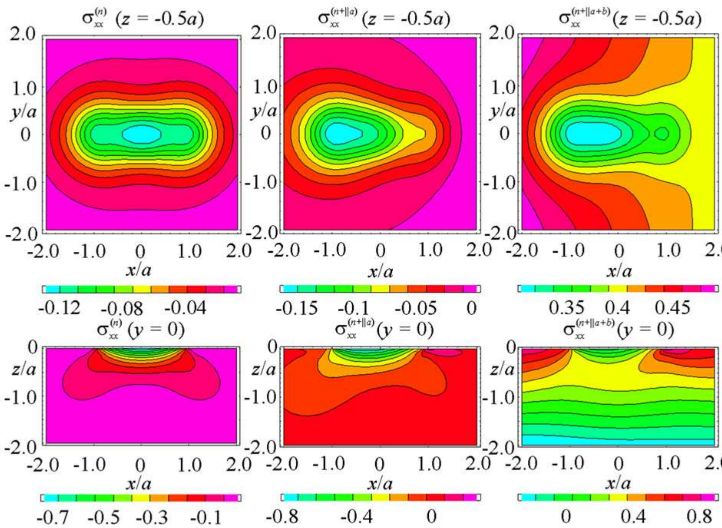

Fig. 5. Comparison of the stress fields σ_{xx} based on p_0 in the tribo-fatigue system

Based on Figure 5 the following conclusions can be made. The influence of non-contact stresses on the change of stress state in the contact region means that

a) the σ_{xx} stresses distribution moves irregularly in the $y = 0$ plane, just according to the value of stresses due bending that change linearly along the z coordinate;

b) the field of compressive stresses is partially transformed to the field of tensile stresses $\sigma_{xx}^{(n+||a+b)}$, where n denotes the action of normal contact pressure, $||a$ denotes the action of tangential forces parallel to half-axis a of contact ellipse, b denotes the action of non-contact bending force.

The analysis of the stress state in the $z = -0.5a$ plane results in the similar conclusions about the influence of non-contact stresses on the change of stress state in the contact region.

a) the σ_{xx} stresses distribution moves irregularly by a value of tribo-fatigue bending stresses in this plane;

b) the field of compressive stresses is partially transformed to that of tensile stresses.

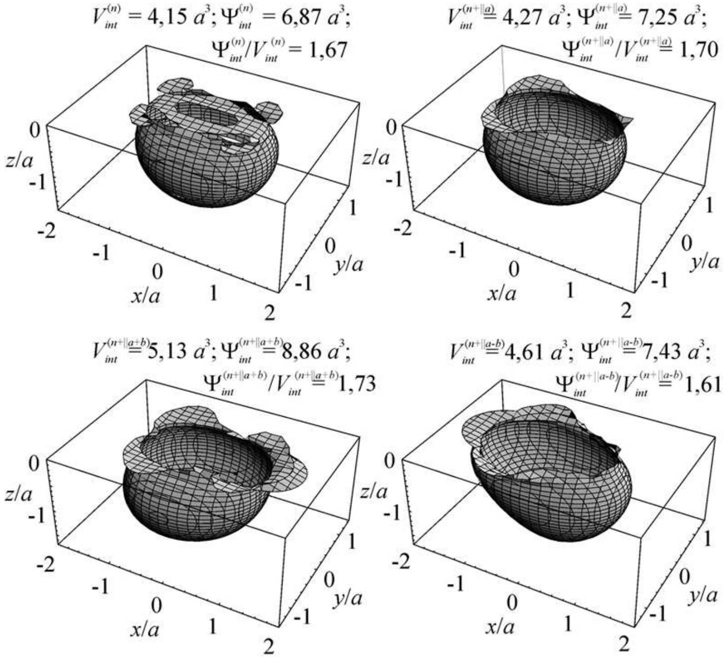

Fig. 6. Dangerous volumes $V_{\text{int}}^{(n)}$, $V_{\text{int}}^{(n+\tau+b)}$, at $\sigma_{\text{int}}^{*\text{lim}} = 0.186p_0$, $f = 0.2$, $b/a = 0.5$

Figure 6 presents the dangerous volumes V_{int} and their damageability Ψ_{int} for different loads. The calculation data are the same as those for the construction of Figure 5 (except the value of F_b in this case was taken as equal to $0.54p_0\frac{(1+\nu)J}{12r^2}$).

It is seen from Figure 6 that as compared to the contact interaction with no friction, the action of tangential forces increases the dangerous volume V_{int} by about 3% and the damageability Ψ_{int} by about 5%. If the shaft is additionally bent due to a non-contact load, then in the tension zone V_{int} still increases by about 20% and the damageability Ψ_{int} by about 22%, whereas in the compression zone they increase by 8% and 3%, respectively.

7. Clamp-knife-base multielement system

Consider an applied problem of assessment of the clamp-knife-base system stress-strain and damageability states (Figure 7a). This system being the part of a cutting instrument is one of the most loaded and critical elements of an agricultural harvester. It is a typical tribo-fatigue system [14, 30, 39] loaded with a bending force applied to the cutting knife, as well as with contact forces due to the compressive bolted connections. One of the directions of this system improvement works being carried out at the Production Association "Gomselmash" is to replace imported steel knives by those made of ВЧТГ cast iron. This iron of home development has high strength (up to 1500 MPa) and plastic (relative extension up to 4%) characteristics. Application of the new material for manufacturing knives has caused the urgency of the task of assessment of a stress-strain state of the clamp-knife-base system with regard to friction force and contact inter-actions between system elements.

Geometric characteristics and the loading condition of the clamp-knife-base system are illustrated in Figure 7a. The base and also the right knife face for modeling the absence of horizontal knife displacements due to bolted connections are rigidly fastened. Resolving equations (12) with the absence of mass forces and boundary element method will be adopted for calculation of the stress-strain state and the damage state of the system in the two-dimensional statement for a uniformly distributed cutting load along the knife that models the cutting of a thick layer of green mass.

Figure 7a demonstrates the stress field distributions in the elements of the clamp-knife-base system for cast iron knife. From this figure it is seen that the stresses σ_{xx} attain their maximum values in two regions: in the vicinity of the knife blade edge where cutting load is applied and in the bolted connection area (clamp upper surface and base lower surface). The analysis of the stresses σ_{xx} shows that in the vicinity of contact between the clamp and the knife the clamp surface undergoes extension and the knife surface -– compression due to the bending by the cutting force.

Qualitatively, the stress-strain state of the system for a steel knife is similar to the one for a cast iron knife. A joint analysis of stress and strain distributions in cast iron and steel knives shows that the material properties of knife changes essentially the stress-strain state of the system. For example, the maximum stresses σ_{xx} and the stress intensity σ_{int} are by approx. 10% and 20% smaller, respectively, in the cast iron knife as against the steel one. On the other hand, the strains ε_{xx} and the strain intensity ε_{int} are to the same extent larger in the steel knife. This effect as a whole corresponds to an approximately 20%th difference in the elasticity moduli of steel and cast iron.

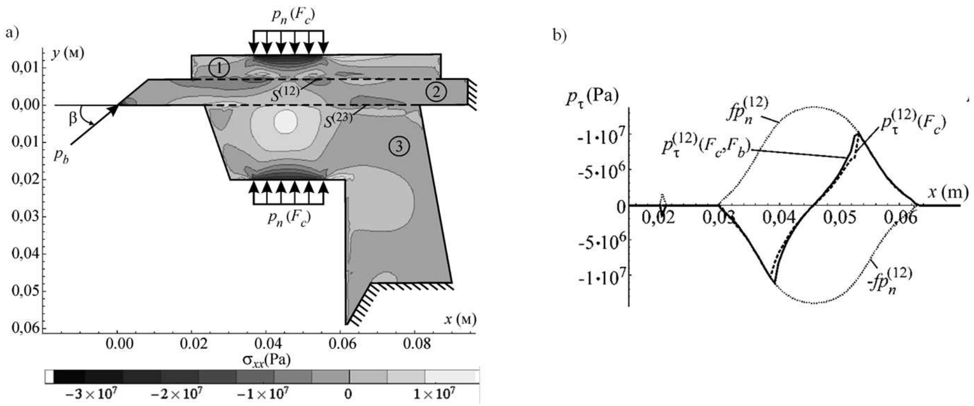

Fig. 7. Clamp-knife-base system: calculation scheme and σ_{xx} stresses distribution (a), tangential tractions between the knife and base (b) at loads $p_b = 16.475$ KN and $p_n = 48.4$ MPa

The analysis of contact interaction in the system can be made using Figure 7b. It shows that the bending non-contact cutting load results in a considerable change in contact pressure and tangential tractions (friction force), i.e. the realization of tribo-fatigue back effect [14, 21, 22, 30]. At the contact surfaces between the clamp and the knife, as well as between the knife and the base the cutting load causes actual contact to reduce.

Moreover, due to the knife bending at the left boundary of the contact surface between the clamp and the knife, contact pressure and tangential forces increase sharply. In essence, this region is the point of knife rotation about the clamp.

While cutting green mass the knife is operating in sliding fatigue conditions. To assess damage one uses a limiting value of the specific friction force $\tau_W^{\lim}$. From works [30, 31] it is known that in the metal-polymer contact pair, which is most close in the interaction parameters of the knife and green mass, the limiting contact pressure p_a ranges as follows: 5 MPa$\leq p_a \leq$ 15 MPa.

The friction coefficient value was chosen as equal to 0.58. It is characteristic for grass, hay, and sunflower. Thus, the limiting values of the specific friction force will be $\tau_W^{\lim} = f_s p_a = 0.58 p_a$.

As the stress intensity σ_{int} with the accuracy up to the multiplier corresponds to maximum tangential (octahedral) stresses, the local damage of the knife operating in frictional fatigue conditions according to is assessed by the relation $\psi_{int} = \sigma_{int}/\tau_W^{\lim}$.

To construct integral characteristics of damage of the knife's material one uses the octahedral dangerous volume V_{int}, the dangerous volume damage Ψ_{int}, $\Psi_{int}^{(V_{av})}$.

Figure 8a shows the distribution of the local damageability ψ_{int} in the cast iron knife as a function of limiting stress. According to Figure 8b for $p_b = 16.475$ KN/m and $p_n = 48.4$ MPa, when limiting stresses $\tau_W^{\lim}$ are increased between 2.9 and 8.7 MPa modeling different types of green mass the value of the knife damageability Ψ_{int}, decrease by a factor of 36. The values of the knife dangerous volume V_{int} and the maximum damage $\psi_{int}^{\max}$ decrease by a factor of 27 and 2.5, respectively.

It is seen from the obtained data that the damageability of the cast iron knife is essentially less than that of the steel one. So, the value of the iron knife dangerous volume V_{int} and also of the dangerous volume damage Ψ_{int} is by approx. 33% less, whereas the value of the maximum damage $\psi_{int}^{\max}$ is by approx. 6% less than that of the steel knife. The lower damage of the cast iron knife could be explained by its lower stress intensity σ_{int} due to the difference of steel and cast iron elasticity moduli metioned above.

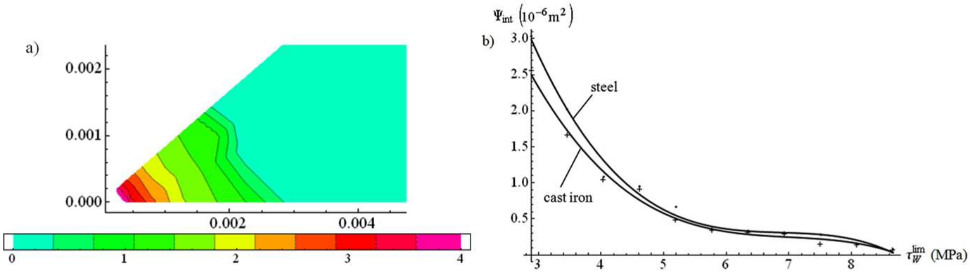

Fig. 8. Distribution of the cast iron knife local damageability ψ_{int} at $\tau_W^{\lim} = 2.9$ MPa (a) dangerous volume damageability Ψ_{int} (b)

Boundary element modeling of the multielement tribo-fatigue clamp-knife-base system has shown that the stress-strain state as a whole and the contact tractions distribution are defined by the joint action of contact and non-contact loads.

Analysis of the two-dimensional model damageability evidences that under other parameters being equal, the use of cast iron knives is more preferred over steel ones in the knife-clamp system since the damageability of the cast iron knife reduces considerably (by approx. 33 %) in comparison with that of the steel one.

8. Conclusions

The methodology of sequential statement and solution of problems of determining the spatial stress-strain state, volume damageability state, and multicriterial states of deformable systems which simultaneously experience the action of volume deformation under tension-compression or bending and local loading under contact interaction with friction is developed.

The system of resolving integral equations is constructed for the system of interacting n bodies subject to mixed boundary conditions. It is based on the model of a zonally homogeneous continuum and allows the interaction of bodies to be modeled in terms of the unknown beforehand contact surfaces including slip and stick subregions.

The model of volume damageability states of tribo-fatigue systems is developed. It is based on the generalized concept of the probabilistic damageability measure called the dangerous volume. Dangerous volume is used to forecast the zones of possible initiation and primary formation of cracks. It allows the characteristics of absolute and relative volume damageability to be defined for the stress-strain state in terms of the parameters of stress intensity, potential deformation energy and stress tensor components.

The theory of multicriterial limiting states of tribo-fatigue systems for the three-dimensional stress-strain state is constructed. It enables one to take into consideration force, temperature and friction loads and to describe failures of system elements in terms of different indicators of the limiting state: volume destruction – splitting into parts; surface destruction – limiting wear. In the particular case of thermal and force loading this theory showed high correlation with a broad range of experimental data.

The regularities of the influence of the local contact interaction on the changes in the stress-strain state and the damageability of a volumetrically deformed element (direct effect) of the system as well as the influence of a non-contact loading on the change of contact interaction characteristics (back effect) confirmed by the wear-fatigue tests were found.

The statement and solution of the applied boundary problems for the multielement clamp-knife-base system of a cutting instrument of an agricultural harvester were made by the finite element method. When solving such problems the knife cutting green mass and the bolted clamping were taken into account. The numerical analysis of the formation of the surfaces of contact interaction between the clamp and the knife, between the knife and the base was made depending on the values of cutting and bolted clamping forces, as well as on knife materials. The stress-strain state and the system volume damageability state were calculated showing the possibility to replace imported steel knives by domestic ones manufactured from high-strength cast iron.

Bibliography

1. Babitsky V.I.: *Theory of Vibro-Impact Systems and Applications*. Springer, 1998.
2. Banerjee P.K., Butterfield R.: *Boundary Element Methods in Engineering Science*. McGraw-Hill, 1981.
3. Beer G., Smith I., Duenser C.: *The Boundary Element Method with Programming: For Engineers and Scientists*. Springer, 2010.
4. Li J., Berger E.J.: *A Boussinesq-Cerruti solution set for constant and linear distribution of normal and tangential load over a triangular area*. J. Elast. **63** (2001), 137–151.
5. Davis R.O., Selvadurai A.P.S.: *Elasticity and geomechanics*. Cambridge University Press, 1996.
6. González J., Abascal R.: *Efficient stress evaluation of stationary viscoelastic rolling contact problems using the boundary element method: Application to viscoelastic coatings*. Eng. Anal. Bound. Elem. **30** (2006), 426–434.
7. Gorshkov A.G., Medvedskiy A.L., Rabinskiy L.N, Tarlakovskiy D.V.: *Waves in continuous media*. Fizmatlit, Moscow 2004 (in Russian).
8. Johnson K.L.: *Contact Mechanics*. Cambridge University Press, 1985.

9. Ma K., Fan S. Xiao J.: *A BEM solution for plates on elastic half-space with unilateral contact*. Eng. Anal. Bound. Elem. **23** (1999), 189–194.
10. Mityushev V.V., Rogosin S.V.: *Constructive Methods for Linear and Nonlinear Boundary Value Problems for Analytic Functions. Theory and Applications*. Chapman &Hall / CRC, Boca Raton 1999.
11. Rabotnov Y.N.: *Mechanics of deformable solids*. Nauka, Moscow 1988 (in Russian).
12. Segonda D., Tafreshi A.: *Stress analysis of three-dimensional contact problems using the boundary element method*. Eng. Anal. Bound. Elem. **22** (1998), 199–214.
13. Shcherbakov S.S.: *Modeling of the damaged state by the finite-element method on simultaneous action of contact and noncontact loads*. Journal of Engineering Physics and Thermophysics **85** (2012), 472–477.
14. Sherbakov S.S., Sosnovskiy L.A.: *Mechanics of tribo-fatigue systems*. BSU Press, Minsk 2011 (in Russian).
15. Sherbakov S.S., Zhuravkov M.A.: *Interaction of Several Bodies as Applied to Solving Tribo-Fatigue Problems*. Acta Mechanica **224** (2013), 1–13.
16. Sherbakov S.S.: *Methods of the analysis wheel/rail laboratory model stress state*. Zavodskaya Laboratoriya. Diagnostika Materialov **11** (2007), 32–40 (in Russian).
17. Shcherbakov S.S.: *Spatial stress-strain state of tribofatigue system in roll–shaft contact zone*. Strength of Materials **45** (2013), 35–43.
18. Shcherbakov S.S.: *State of Volumetric Damage of Tribo-Fatigue System*. Strength of Materials **45** (2013), 171–178.
19. Shcherbakov S.S.: *Stress-strain state of disk/cylinder system in conditions of contact interaction and cylinder bending*. Vesti NANB. Physical and technical sciences series **3** (2010), 29–34 (in Russian).
20. Shcherbakov S.S.: *Three-dimensional stress-strain state of a pipe with corrosion damage under complex loading*. In: Tribology – Lubricants and Lubrication, Chang-Hung Kuo (ed.). InTech, Rijeka 2011, 139–172.
21. Sosnovskii L.A., Komissarov V.V., Shcherbakov S.S.: *A method of experimental study of friction in a active system*. Journal of Friction and Wear **33** (2012), 136–145.
22. Sosnovskii L.A., Komissarov V.V., Shcherbakov S.S.: *Comparative experimental study of friction parameters in a tribopair and a force system*. Journal of Friction and Wear **33** (2012), 258–264.
23. Sosnovskiy L.A., Bogdanovich A.V., Yelovoy O.M., Tyurin S.A., Komissarov V.V., Shcherbakov S.S.: *Methods and main results of Tribo-Fatigue tests*. International Journal of Fatigue **66** (2014), 207–219.
24. Sosnovskiy L.A., Shcherbakov S.S.: *Mechanothermodynamical system and its behavior*. Continuum Mech. Thermodyn. **24** (2012), 239–256.
25. Sosnovskiy L.A., Shcherbakov S.S.: *Mechanothermodynamic Entropy and Analysis of Damage State of Complex Systems*. Entropy **18** (2016), 268.
26. Sosnovskiy L.A., Shcherbakov S.S.: *Mechanothermodynamics*. Springer, 2016.
27. Sosnovskiy L.A., Shcherbakov S.S.: *Special Class of Contact Problems and the Calculation of the State of Stress of Wheel / Rail System Elements*. In: Proc. of the 7th International Conference on Contact Mechanics and Wear of Rail/Wheel Systems. Brisbane **1** (2006), 115–125.
28. Sosnovskiy L.A., Shcherbakov S.S.: *Surprises of Tribo-Fatigue*. Magic Book, Minsk 2009.
29. Sosnovskiy L.A., Shcherbakov S.S.: *Vibro-impact in rolling contact*. J. of Sound and Vibration **308** (2007), 489–503.
30. Sosnovskiy L.A.: *Tribo-Fatigue. Wear-fatigue Damage and Its Prediction*. Springer, Berlin 2005.
31. Sosnovskiy L.A., Zhuravkov M.A., Sherbakov S.S.: *Fundamental and Applied Problems of Tribo-Fatigue: Course of Lectures*. BSU Press, Minsk 2011 (in Russian).
32. Sutradhar A., Paulino G., Gray L.J.: *Symmetric Galerkin Boundary Element Method*. Springer, Berlin 2008.
33. Triantafyllidis T.: *3-D time domain BEM using half-space Green's functions*. Eng. Anal. Bound. Elem. **8** (1991), 115–124.
34. Vrettos C.: *Green's functions for vertical point load on an elastic half-space with depth-degrading stiffness*. Eng. Anal. Bound. Elem. **32** (2008), 1037–1045.
35. Wang C.D., Liao J.J.: *Elastic solutions for a transversely isotropic half-space subjected to arbitrarily shaped loads using triangulating technique*. Int. J. Geomech. **1** (2001), 193–224.

36. Yang B., Pan E., Tewary V.K.: *Three-dimensional Green's functions of steady-state motion in anisotropic half-spaces and biomaterials*. Eng. Anal. Bound. Elem. **28** (2004), 1069–1082.
37. Zhuravkov M.A.: *Fundamental solutions of the elasticity theory and some of their applications in geomechanics of soils and bases*. BSU Press, Minsk 2008 (in Russian).
38. Zhuravkov M.A., Martynenko M.D.: *Theoretical fundamentals of strain mechanics of the rock salt block-layered massif*. Universitetskoye Press, Minsk 1995 (in Russian).
39. Zhuravkov M.A., Sherbakov S.S., Krupoderov A.V.: *Modeling of volumetric damage of multielement clamp-knife-base tribo-fatigue system*. Z. Angew. Math. Mech. (ZAMM) **97** (2017), 60–69.